

Facial Asymmetry: A New Biometric

Y. Liu, R. L. Weaver^a, K. Schmidt^b, N. Serban^a, J. Cohn^b

CMU-RI-TR-01-23

^aStatistics Department, Carnegie Mellon University

^bDepartment of Psychology, University of Pittsburgh

The Robotics Institute
Carnegie Mellon University
Pittsburgh, PA 15213

ABSTRACT

Human facial asymmetry has long been a critical factor for evaluations of attractiveness and expressions in psychology and anthropology, although most studies are carried out qualitatively. In this work, we investigate in depth the effect of statistical facial asymmetry measurement as a biometric under expression variations. Our findings demonstrate that the asymmetry of specific facial regions captures individual differences that are robust to variation in facial expression. More importantly, our experimental results show that facial asymmetry provides discriminating power orthogonal to conventional face identification methods. The synergy of combining facial asymmetry with conventional methods is evaluated. Our work appears to be the first to show quantitatively the power of facial asymmetry as a biometric.

1 Motivation

Human facial asymmetry has long been a critical factor for evaluation of facial attractiveness [16], and expressions [15] in psychology and anthropology, albeit most studies are carried out qualitatively using human observers as judges.

Intrinsic facial asymmetry in individuals is affected by multiple factors, including growth, injury, and age-related change. The asymmetry of a face is an individualized characteristic, differing in perceptible ways even between identical twins [13]. Facial asymmetries are explained as the result of slight disruptions in development [16]. Individuals in the general population display a



Figure 1: *Left: original face. Middle: a perfectly symmetrical face made of the left half of the original face. Right: a perfectly symmetrical face made of the right half of the original face. Notice the difference in nose regions in both individuals caused by left-right asymmetry.*

wide range of variation in the amount of facial asymmetry (Figure 1), as well as in the rest of the

body. Asymmetrical faces are considered less attractive [16]. It has been reported that facial attractiveness for men is inversely related to recognition accuracy [14]. These results imply a positive relationship between facial asymmetry and recognition rates.

Humans have an amazing sensitivity to naturally occurring facial asymmetry in face recognition. A small yet statistically significant decrease in recognition performance is observed when facial asymmetry is removed from images [17]. This suggests that explicit representation of facial asymmetry may enhance automatic face recognition tasks as well, especially under expression variations. Though qualitative measures of face asymmetry are shown to be behaviorally relevant [4], very little research has been aimed at a quantitative study of facial asymmetry [15], and none that we can find has studied the relationship between facial asymmetry and face identification under expression variations. In particular, it is not clear if facial asymmetry is characteristic to people or to expressions.

Extrinsic facial asymmetry is caused by viewing orientation, illuminations, shadows, and highlights. In this paper, we investigate in depth the effect of statistical facial asymmetry measurement as a biometric under expression variations with minimal extrinsic factors, though at the end of this paper we will show an example of using facial asymmetry to determine best pose. Our goal in this paper is to find out whether inherent facial asymmetry is discriminating across different individuals with varied facial expressions.

(A)symmetry is a holistic property of a form that our visual system focuses on preattentively to detect equivalence in shape. Facial asymmetry is especially relevant in face identification from a distance, where detailed facial features may be blurred and structural features of the face play a more important role.

Human faces are approximate bilateral symmetric. However, facial **asymmetry** is well established in comparative psychology [8]. This discrepancy poses the following questions: *Can human faces' departure from perfect bilateral symmetry be quantitatively measured? Does this measurement provide useful information for human identification?* It is within this narrow, yet quantifiable margin between perfect-symmetry and natural facial asymmetry, that a facial asymmetry-based analysis can demonstrate its discriminating power. So far, no human face has been found to be perfectly symmetrical. The approach we take treats facial asymmetry as a continuous, multidimensional statistical feature.

For the purpose of classification and clustering, anatomical (a)symmetry of humans and animals has been exploited successfully in other fields [12, 2, 10, 11, 5, 8]. An analogy can be made here between human brains and faces. The anatomical structures of normal human brains systematically differ from perfect symmetry [7, 6]. In [11], using statistical asymmetry measurements from images of normal and pathological human brains alone, an average of 80% precision rate is

achieved for neural pathology discrimination.

2 Quantification of Facial Asymmetry

Asymmetry is a structural descriptor of an object that cannot be captured by a single local measure. Bilateral reflection symmetry is defined with respect to a reflection line/plane, and human faces possess such a natural reference line/plane.

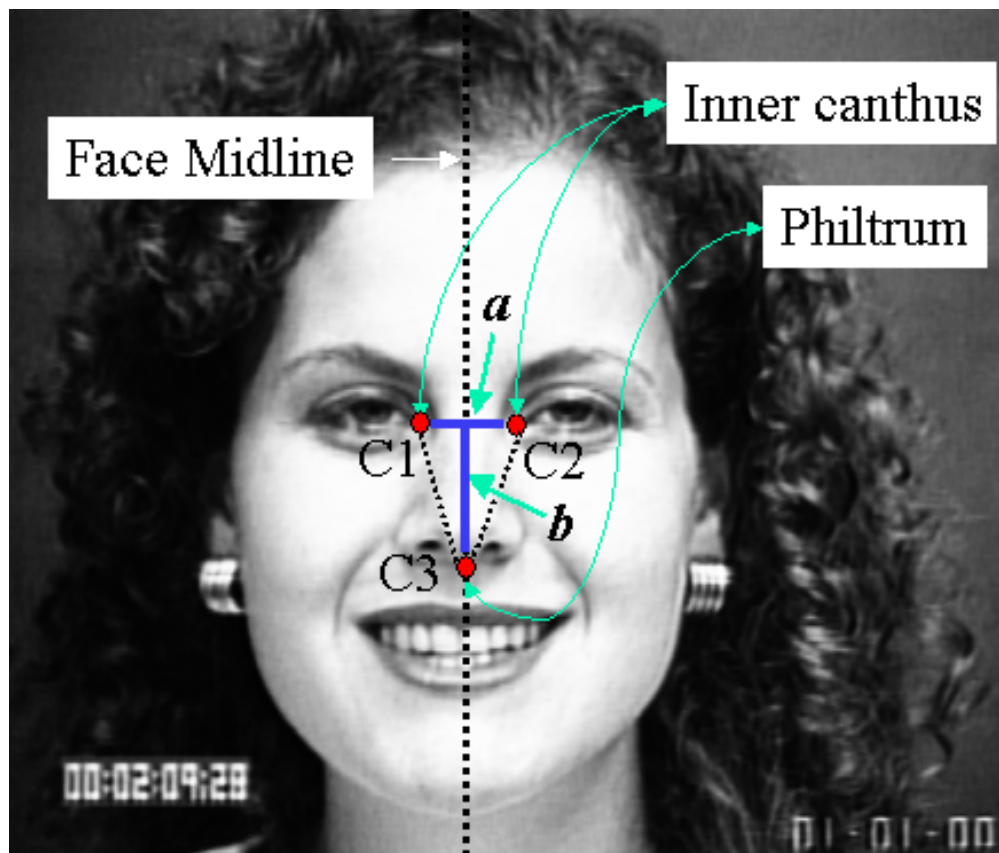


Figure 2: Each face image is normalized using three points: left and right inner canthus (C_1, C_2) and the philtrum (C_3), by (1) rotate $C_1\bar{C}_2$ into a horizontal line segment, (2) scale $C_1\bar{C}_2$ into length a , (3) skew the face image horizontally such that C_3 is located on the midline of C_1, C_2 , (4) scale the distance between C_3 and $C_1\bar{C}_2$ to length b .

2.1 Face Image Normalization

We define a *face triangle* as the one formed by connecting three points: the inner canthus of each eye, (C_1, C_2) , and the philtrum C_3 (Figure 2). Each face image is *normalized* using these three points by an affine deformation: (1) rotation: rotate $C_1\bar{C}_2$ into a horizontal line segment, (2) X-scaling: scale $C_1\bar{C}_2$ into length a , (3) X-skewing: skew the face image horizontally such that C_3 is located on the perpendicular line going through the midpoint of C_1, C_2 , (4) Y-scaling: scale the distance between C_3 and $C_1\bar{C}_2$ to length b . The *face midline* is defined as the line going through the mid point of $C_1\bar{C}_2$ and C_3 . Each image is cropped into a 128×128 squared image with face midline centered vertically. The three points C_1, C_2 and C_3 were found in real expression video sequences by hand-selecting three points on the first frame and then automatically tracking the rest of the video frames, with the results verified and corrected afterwards by a human user. The resulting normalized face is an affinely deformed and cropped image of the original. The net effect of this deformation is to normalize each face with respect to its own face midline (*face triangle*) (Figure 2). All normalized faces have their inner canthus and the philtrum on the same pixel locations. In our experiment these three points are: $C_1 = [40, 48], C_2 = [88, 48]$ and $C_3 = [64, 84]$, thus $a = 48$ and $b = 36$ respectively (upper-left corner has coordinates $[0,0]$) (Figures 2 and 3).

2.2 Facial Asymmetry Measurements

Once a face midline is determined, each point on the normalized face image has a unique corresponding point on the other side of the face image (given even number of columns in the image). For a given normalized face density image I , a coordinate system defined on the face with X axis perpendicular to the face midline and Y axis coincides with the face midline, its vertically reflected (w.r.t. axis Y) image I' , and their respective edged images I_e, I'_e , we can define the following two facial asymmetry measurements

Density Difference D -face:

$$D(x, y) = I(x, y) - I'(x, y) \quad (1)$$

Edge Orientation Similarity S -face:

$$S(x, y) = \cos(\phi_{I_e(x,y), I'_e(x,y)}) \quad (2)$$

Figure 4 displays three normalized faces, and their respective D -face and S -face. We call these *AsymFaces*. S -face is bilaterally symmetrical, and the left and right of D -face are opposite of each other. Therefore, the left half of D - and S -faces contains all the information needed. We denote these half faces as \mathbf{D}_h and \mathbf{S}_h with dimension 128×64 . See Table 1 for a complete set of notations used in the rest of this paper.



Figure 3: Normalized expressions (joy, anger, disgust) from Cohn-Kanade AU-Coded Facial Expression Database [9]. Each column represents one subject (total of 7 subjects displayed) at neutral, peak joy, peak disgust and peak anger expression video sequences, respectively.

Notation	Definition	Size
D-face	Intensity Difference image	128×128
S-face	Edge Orin. Similarity image	128×128
\mathbf{D}_h	Left half of D-face	128×64
\mathbf{S}_h	Left half of S-face	128×64
D_{hx}	column-mean of \mathbf{D}_h on X	1×64
D_{hy}	row-mean of \mathbf{D}_h on Y	128×1
S_{hx}	column-mean of \mathbf{S}_h on X	1×64
S_{hy}	row-mean of \mathbf{S}_h on Y	128×1
SD_{hx}	smoothed D_{hx}	1×64
SD_{hy}	smoothed D_{hy}	128×1
SS_{hx}	smoothed S_{hx}	1×64
SS_{hy}	smoothed S_{hy}	128×1
DataSet 1	60 PCA on \mathbf{D}_h of 55 subjects 3 frames from each exp. seq.: neutral, middle, peak	60×495
DataSet 2	SD_{hy} of all distinct frames of 55 subjects	128×2677
DataSet 3	S_{hy} of all distinct frames of 55 subjects	128×2677

Table 1: Terms for different AsymFaces are defined. Datasets for face recognition experiments are also defined.

These two asymmetry measurements capture facial asymmetry from different perspectives; *D-face* is affected by the left-right relative intensity variations of the face while *S-face* is affected by the zero-crossing of the intensity field. The higher the value of *D-face* the more *asymmetrical* the face, and the higher the value of *S-face* the more *symmetrical* the face.

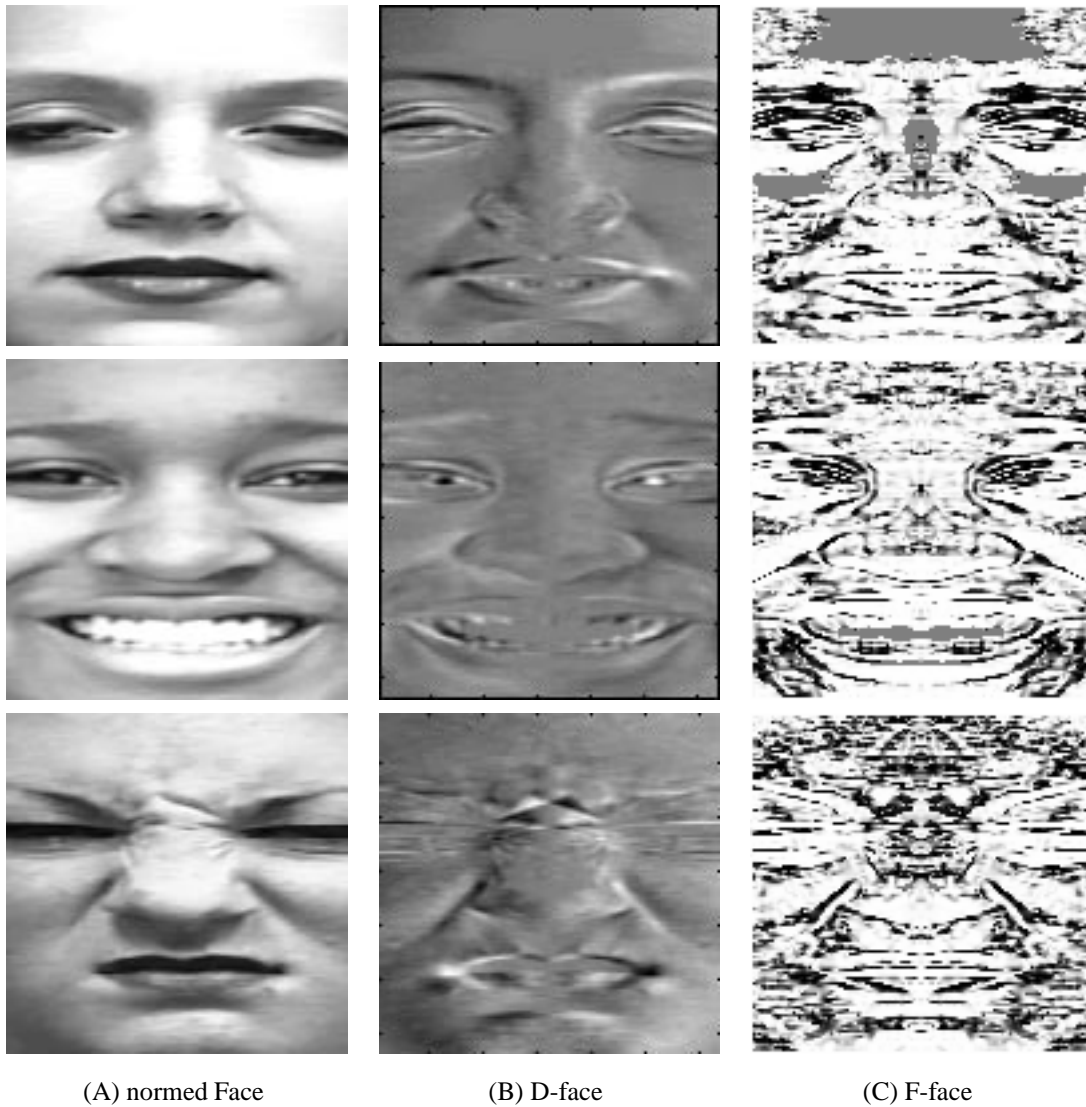


Figure 4: (A) *normalized face* , (B) *D-face*, and (C) *F-face*.

3 Facial Expression Image Data

The Cohn-Kanade AU-Coded Facial Expression Database [9] is used to investigate the relationship between facial asymmetry and recognition. This dataset consists of video sequences of different subjects of different races displaying distinct facial expressions, such as anger, disgust or joy. There are three variations in lighting: 1) ambient lighting, 2) a single high intensity lamp, 3) dual high intensity lamps with reflective umbrellas. Video sequences range in length from 8 to 65 frames, and each frame is a grey-scale image of 640x480 pixels.

As an initial attempt, we use frontal facial images which have the least lighting distortions. This is for the purpose of isolating the intrinsic from extrinsic factors, and finding out how these intrinsic facial asymmetry may contribute to human identification under facial expression variations alone. We have experimented with human identification using a random subset of the dataset on 55 subjects, each with 3 expression video sequences: joy, anger and disgust. After manually removing redundant frames in each sequence such that adjacent frames provide significant visual variations, a total of 2677 frames is left with 922 for joy, 945 for anger and 810 for disgust.

Figure 5 shows the average *D-face* (*S-face*) from 55 subjects and its most asymmetrical (symmetrical) regions. Figure 6 demonstrates the \mathbf{D}_h means along X and Y axes respectively, D_{hx} and D_{hy} . One can observe from these plots which rows and columns of the face in average are most asymmetrical (symmetrical).

4 Feature Space Dimension Reduction

Each *AsymFace* \mathbf{D}_h or \mathbf{S}_h has 8192 ($128 \times 64 = 8192$) dimensions (Table 1). Not all these dimensions are independent of each other. In order to (1) better understand the facial asymmetry measures, (2) reduce the cost of computation, and (3) increase classification accuracy, we have experimented with several ways to reduce the dimensionality of the *AsymFaces*.

4.1 Principle Component Analysis

PCA is done on an 8192×495 matrix to produce **Dataset 1** defined in Table 1. $8192 = 128 \times 64$ is the total number of pixels in each \mathbf{D}_h , and 495 comes from taking three frames from each of the three expressions of each subject ($3 \times 3 \times 55 = 495$). The three frames from each emotion sequence are chosen from the most neutral, the most peak and the middle frames. After examining the eigen values, the top 60 components are kept. The dimensions are thus reduced from 8192 to 60.

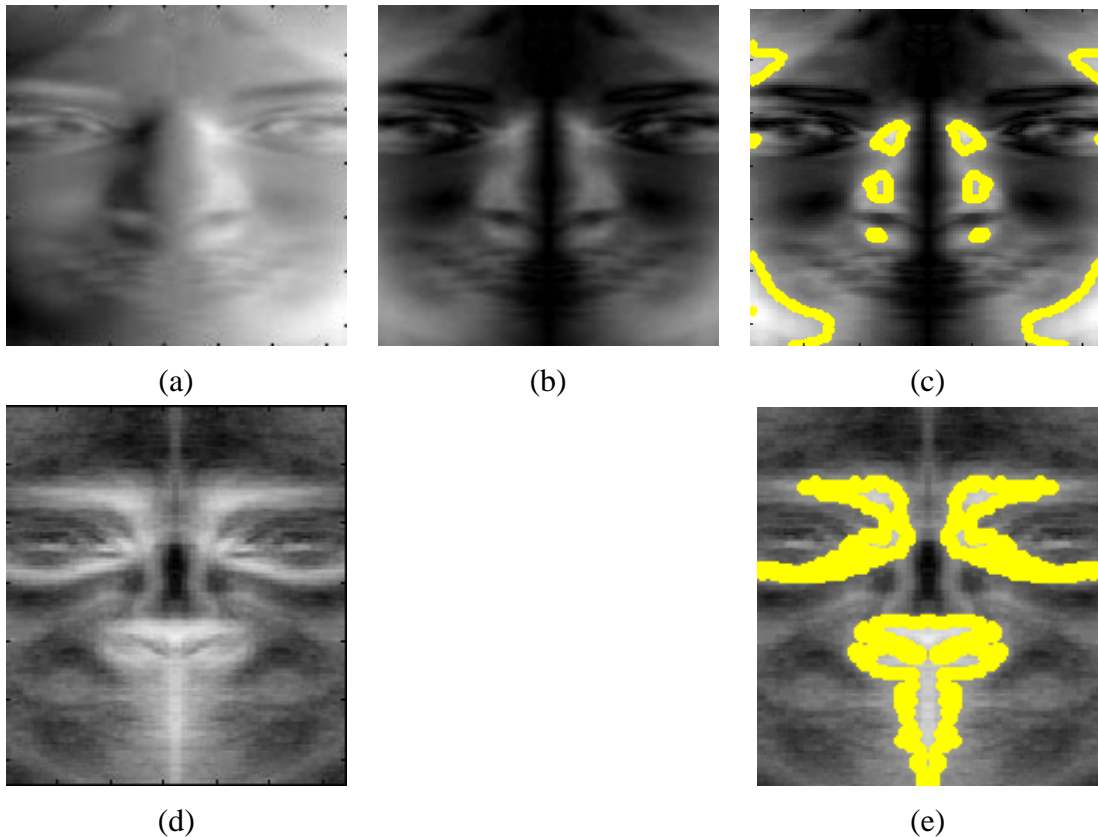


Figure 5: (a) average D-face. (b) the absolute values of D-face (c) the top 1/3 most **asymmetrical** regions by D-face measure are circled. (d) average S-face. (e) the top 1/3 most **symmetrical** regions by S-face measure are circled.

4.2 Feature Averaging

Inspired by plots in Figure 6, we computed the mean values of \mathbf{D}_h : D_{hx} (1×64) and D_{hy} (128×1). Figure 7 shows the smoothed D_{hy} surfaces of video sequences from two distinct subjects, each with three expressions (joy, anger, disgust consecutively). Despite changes in expressions, geometric similarities of each person across different expression sequences and dis-similarity between individuals can be observed.

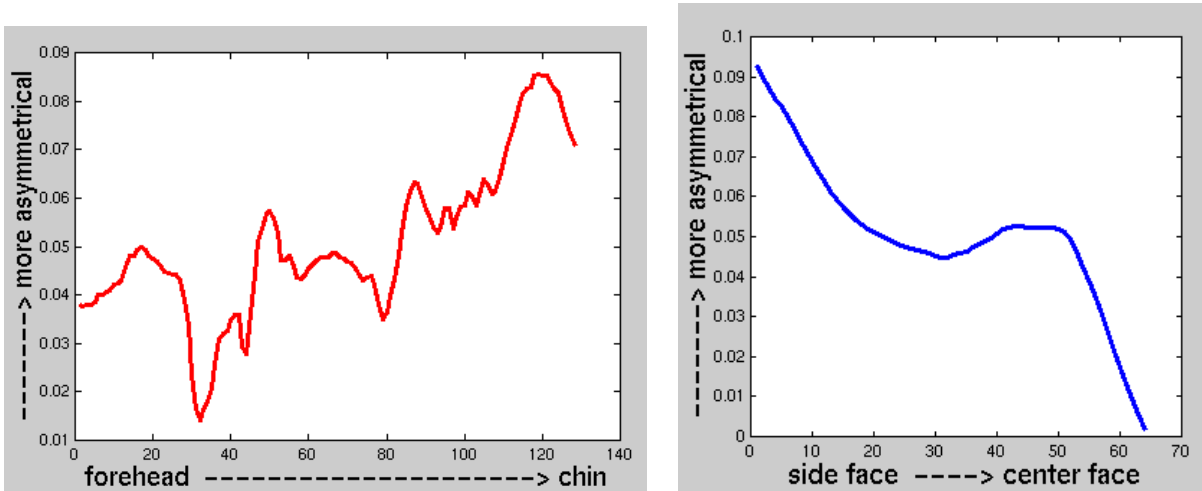


Figure 6: Left: the row-mean (1-128) D_{hy} starting from forehead to chin of the average D-face above. Right: the column-mean (1-64) D_{hx} starting from side of the face (more asymmetrical) to the center of the face (more symmetrical) of the average D-face.

4.3 Discriminative Feature Subset Selection

For a feature F with C total classes, we define a variance ratio as follows

$$vr(F) = \frac{Var(F)}{\frac{1}{C} \sum_{i=1..C} \frac{Var_i(F)}{\min_{i \neq j} (|mean_i(F) - mean_j(F)|)}}$$

where $mean_i(F)$ is the mean of feature F 's values in class i . This variance ratio is the ratio of the variance of the feature between subjects to the variance of the feature within subjects, with an added penalty for features which may have small intra-class variance but which have close inter-subject mean values. Figure 8 shows this ratio for SD_{hy} and its variance. The features that have higher variance ratios are more discriminative. This figure shows which rows among all AsymFaces (**DataSet 2**) are more discriminating than others. The row with the highest value corresponds to the nose bridge region. This is consistent with our observations in Figure 1. The 3 peaks after that are, roughly, at the row levels of mid-forehead, inner-eye corner and between mouth and chin. It is a misconception that the most discriminative individual features form the most discriminative feature subset. We have employed both exhaustive searches and heuristic forward selection [3] searches to find the most discriminating feature subsets from AsymFaces.

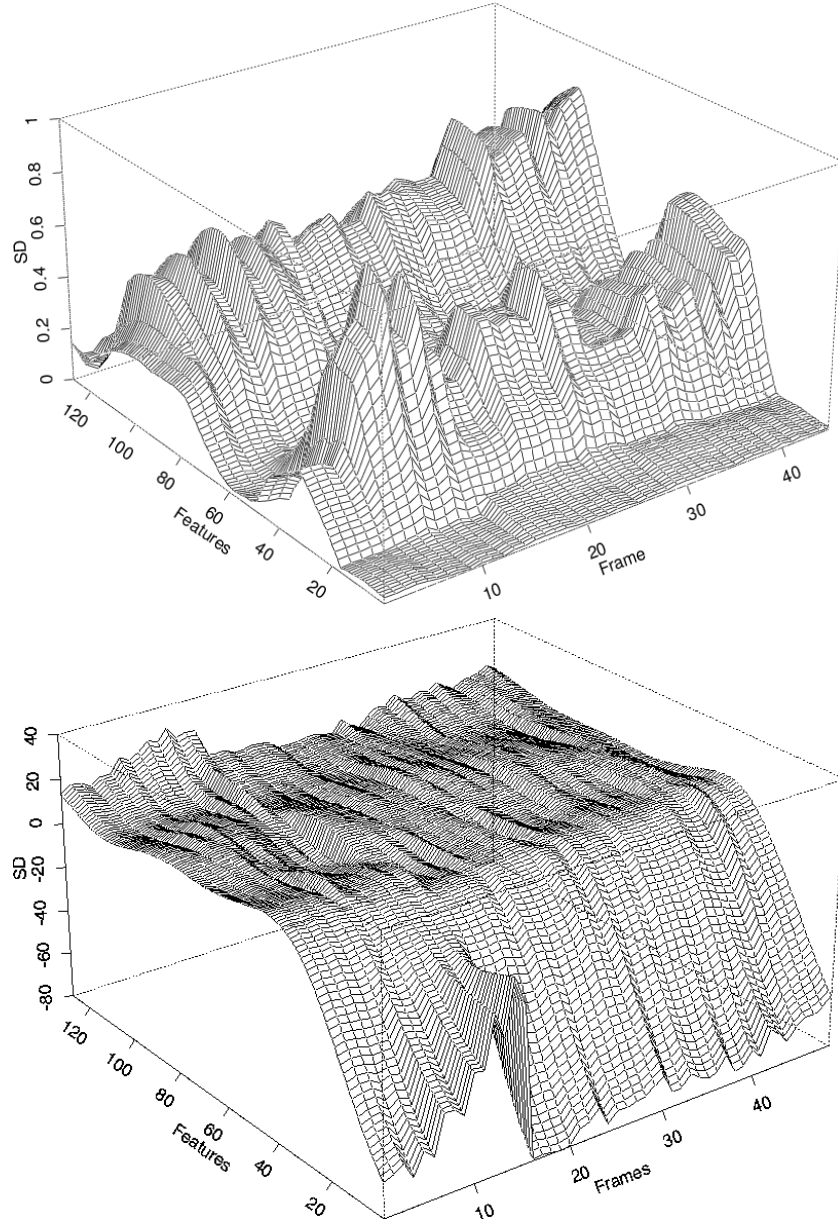
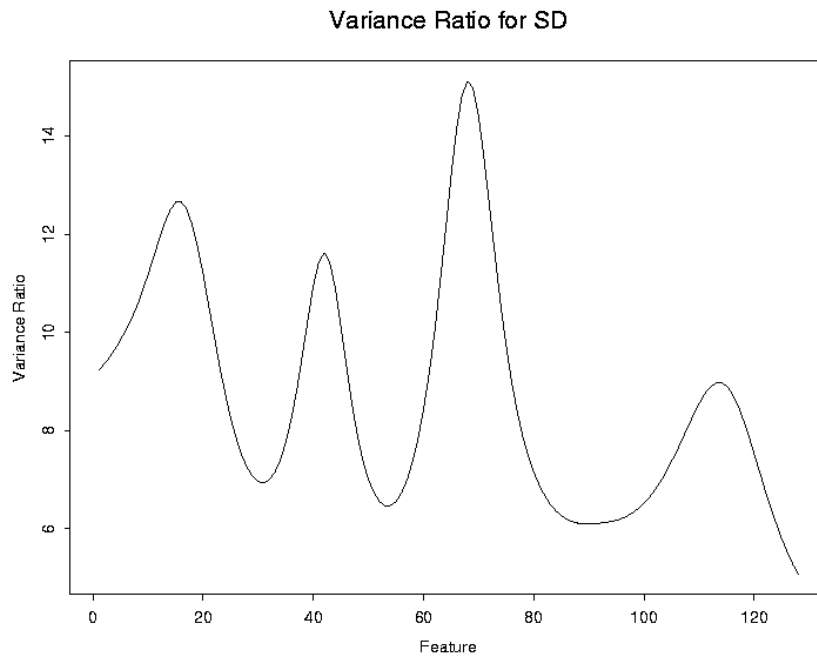
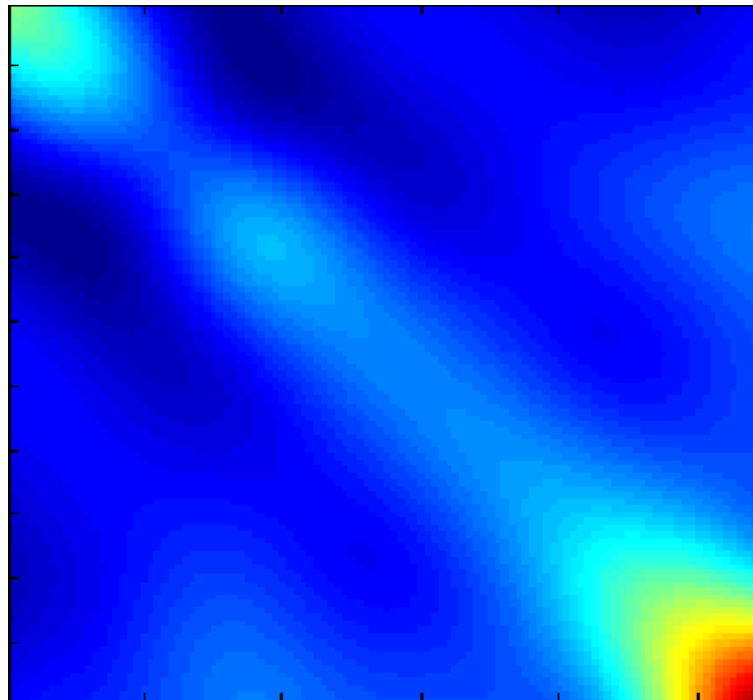


Figure 7: Top: SD_{hy} sheet of subject 85. Bottom: SD_{hy} sheet of subject 10. The three axes in both plots represent, from left-to-right, joy-anger-disgust video frame sequences consecutively; from front to back, each row on the AsymFace SD_{hy} from forehead towards the chin; and the height is the D-face value.



(a)



(b)

Figure 8: (a) The smoothed variance ratio for SD_{hy} of **DataSet 2** shows which rows of the Asym-Face are the most discriminative. From left to right is from forehead to chin. The highest peak is around nose bridge area. (b) The covariance matrix of SD_{hy} shows the asymmetry of the mouth region varies the most.

5 Face Identification

We have designed five basic types of experiments: (1) training on all neutral expression frames and testing on peak expression frames of all three expressions; (2) the inverse of (1); (3) - (5) training on two expressions, and testing on the images from the third unseen expression.

5.1 Linear Discriminant Analysis (LDA) on AsymFaces (AF)

For a data set \mathbf{X} consisting of C classes, the objective of LDA is to obtain a $(C - 1)$ -dimensional linear combination, $Y = A'X$ that maximizes the ratio

$$\frac{A'BA}{A'WA},$$

where B is the variance between groups, and W is the common covariance matrix for features within a single group. The idea behind this condition is to maximize the variance from one group to another and to minimize the variance inside each group.

The classification procedure is an estimate of the optimal rule drawn from the normal population, and it is expected to perform well in samples with large size. The observation X_0 is assigned to class k if:

$$d_k(X_0) = \max(d_i(X_0) : i = 1..C)$$

where

$$d_k(X_0) = -\frac{1}{2}(X_0 - \bar{X}_k)' \Sigma^{-1} (X_0 - \bar{X}_k) + \log(p_k).$$

Here p_k is the prior weighting of group k , and Σ is the common covariance matrix for features within a class. The term in the distance formula, $(X_0 - \bar{X}_k)' \Sigma^{-1} (X_0 - \bar{X}_k)$, is the Mahalanobis distance of the observation X_0 to the centroid of class k , used in maximum likelihood estimation.

Classification rates using LDA on AsymFaces have reached between 70% and 96% on different training/testing setups (Table 2).

5.2 Fisherfaces (FF)

The Fisherfaces method [1] uses the Fisher Linear Discriminant (FLD) to achieve class specific linear projections of the given image set. PCA is done on the original images to reduce the dimension to $C - 1$, where C is the total number of classes. We have implemented this method and tested it on **Dataset 1**. Good results from Fisherfaces are expected since all the images are registered and normalized, the only factor that may cause error is the expression variations. Fisherfaces results can be found in Table 3.

DataSet	AsymFace	Features	Training Data	Testing Data	%Error
1	D_h	top 14 principal components	joy & disgust	anger	26.1%
1	D_h	top 20 principal components	anger & disgust	joy	23.0%
1	D_h	top 14 principal components	joy & anger	disgust	22.4%
1	D_h	top 14 principal components	neutral/middle	peak	13.3%
1	D_h	top 14 principal components	peak/middle	neutral	13.3%
2	SD_{hy}	5,7,6,15,14,11,119,10,116,76,68,19,40 69,13,42,23,24,39,26,56,83,35,75,28	joy & disgust	anger	19.5%
2	SD_{hy}	5,7,6,15,14,11,119,4,2,61,39, 108,56,46,127,17,67	anger & disgust	joy	30.0%
2	SD_{hy}	5,7,6,15,14,11,119,116,76,68,2, 40,69,42,23,118,24,112,39,108,25,1	joy & anger	disgust	25.8%
2	SD_{hy}	5,7,6,15,14,11,8,119,18,116,76,68,2,40 69,42,118,61,56,77,41,60,67,47,70,30,12,45	neutral 2/3	peak 1/3	7.9%
2	SD_{hy}	5,7,6,15,14,11,119,18,10,4,116,76, 68,19,40,69,112,113,22,108,26,56,83,46,21	peak 2/3	neutral 1/3	6.6%
2 + 3	$SD_{hy} \& S_{hy}$	$SD_{hy}(15,18,23,27,39,40,43,46,56,61,68,108,112,119,121)$ $S_{hy}(2:20,50:90,116:128)$	joy & disgust	anger	14.1%
2 + 3	$SD_{hy} \& S_{hy}$	$SD_{hy}(15,18,19,23,27,39,43,61,65,68,108,112,119)$ $S_{hy}(2:20,50:80,116:128)$	anger & disgust	joy	20.7%
2 + 3	$SD_{hy} \& S_{hy}$	$SD_{hy}(14,19,23,40,68,69,76,116)$ $S_{hy}(2:20,50:90,116:128)$	joy & anger	disgust	19.3%
2 + 3	$SD_{hy} \& S_{hy}$	$SD_{hy}(5,7,6,15,8,119,76,68,2,42,68,56)$ $S_{hy}(2:20,50:90,116:128)$	neutral 2/3	peak 1/3	5.2%
2 + 3	$SD_{hy} \& S_{hy}$	$SD_{hy}(5,7,6,15,8,119,76,68,2,42,68,56)$ $S_{hy}(2:20,50:90,116:128)$	peak 2/3	neutral 1/3	4.0%

Table 2: Using AsymFaces alone, sample results of LDA are shown. **Dataset 1** consists of 495 frames from 55 subjects, with each subject having a sequence of 3 frames for each emotion. **Dataset 2 (3)** consists of 2677 frames from 55 subjects with variable numbers of frames per subject, per emotion. See Table 1 for definitions of the AsymFaces metrics.

PCA Face Features	Auto Selected D_h PCA Features	Training Data	Testing Data	Fisherfaces %Error	FF + AF %Error	Improvement Rate
1:10	1,2,9,10,12,13,23,28	joy & anger	disgust	13.3%	3.0%	77.4%
1:15	1,3,4,12,18,20,21,47,60	joy & anger	disgust	8.5%	1.8%	78.8%
1:10	1,2,5,6,8,10	joy & disgust	anger	10.3%	4.8%	53.4%
1:15	1,3,4,10,15,23,46,55	joy & disgust	anger	6.7%	1.8%	73.1%
1:10	1,2,6,12,23,43,48	anger & disgust	joy	27.9%	13.3%	52.3%
1:15	1,2,4,7,14,27,30,43,50	anger & disgust	joy	19.4%	9.7%	50.0%
1:10	1,2,4,7,12,24,28,47	neutral/middle	peak	9.7%	0.6%	93.8%
1:15	2,4,16,19,26	neutral/middle	peak	3.6%	0.0%	100.0%
1:10	1,2,5,6,7,9,17	peak/middle	neutral	8.5%	1.8%	78.8%
1:15	1,15,23	peak/middle	neutral	6.1%	2.4%	60.7%

Table 3: Improved results are shown, in contrast to Fisherfaces (FF) results, when combining Fisherfaces computed from the normalized face images directly with AsymFaces (AF) computed from the eigen vectors of D_h (**DataSet 1** defined in Table 1). In each case, the AF features were chosen according to forward selection with respect to the variance ratio. Improvement rate = $(\%Error(FF) - \%Error(FF+AF))/\%Error(FF)$.

5.3 Combination of FF and AF

When Fisherfaces and AsymFaces are combined using LDA, the Fisherfaces classification errors are reduced by 50% to 100% (0% error). This is done by concatenating both top eigen vectors (1-10, 1-15) directly computed from normalized face images and automatically selected features from AsymFaces, then applying LDA on the five experimental setups (Table 3).

6 Discussion

Using AsymFaces alone, face classification rates are between 70% to 96% (Table 2). Using Fisherfaces alone, the correct classification rates are between 72.1% and 96.3% (Table 3). Combining both the AsymFaces and the Fisherfaces, the face classification rates are increased to between 86.7% and 100% (Table 3). These results, on 55 subjects of different gender, race, and expressions, suggest that AsymFaces are complementary to Fisherfaces for human face identification under expression variations. The results show that, most of the time, the worst accuracy occurs when training on anger and disgust, testing on joy. On further investigation, we have found that the most discriminative AsymFace features for joy *alone* differ from those for anger and disgust,

and from all three expressions considered together. The cause of this difference may come from the fact that joy is the only positive emotion in the three expressions.

7 Conclusion

In this work we have studied the use of facial asymmetry for identification. We have proposed two simple quantitative measures of facial asymmetry and demonstrated that

- D and S AsymFaces are simple and fast to compute (simplicity);
- the asymmetry of specific facial regions captures individual differences and is robust to variation in facial expression, and using AsymFaces alone LDA can achieve comparable face identification accuracy as using Fisherfaces on the same dataset (discriminative);
- significant enhanced classification rates can be achieved by combining AsymFaces with Fisherfaces (orthogonality)

Our results suggest that facial asymmetry contains significant information for human identification under expression variations, that it should not be ignored in automatic face recognition.

Facial asymmetry is not only useful under frontal views. Actually, asymmetry measure can be used for selecting best viewing angles in a sequence of video images. Figure 9 demonstrates such an application for both visual and thermal images of a subject.

Our future work includes examining the effects of extrinsic factors of facial asymmetry (e.g. taking advantage of self-shadowing such as nose), expression identification (temporal variations of facial asymmetry), and effective feature combination schemes for optimal face classification.

This work opens up a novel research subfield in face recognition where facial asymmetry and its quantitative relationship to face identification based on race, gender, age, attractiveness and expressions may be evaluated, and compared with human performance.

8 Acknowledgement

The authors would like to thank Dr. J. Philips of DARPA for productive discussions, and CMU students Dan Bohus (computer science), Marc Fasnacht (physics), and Yan Karklin (computer science) who worked on a subset of the 55 subjects reported in this paper as a class project (Fall 2000) with Dr. Liu. This research is supported in part by ONR N00014-00-1-0915 (HumanID).

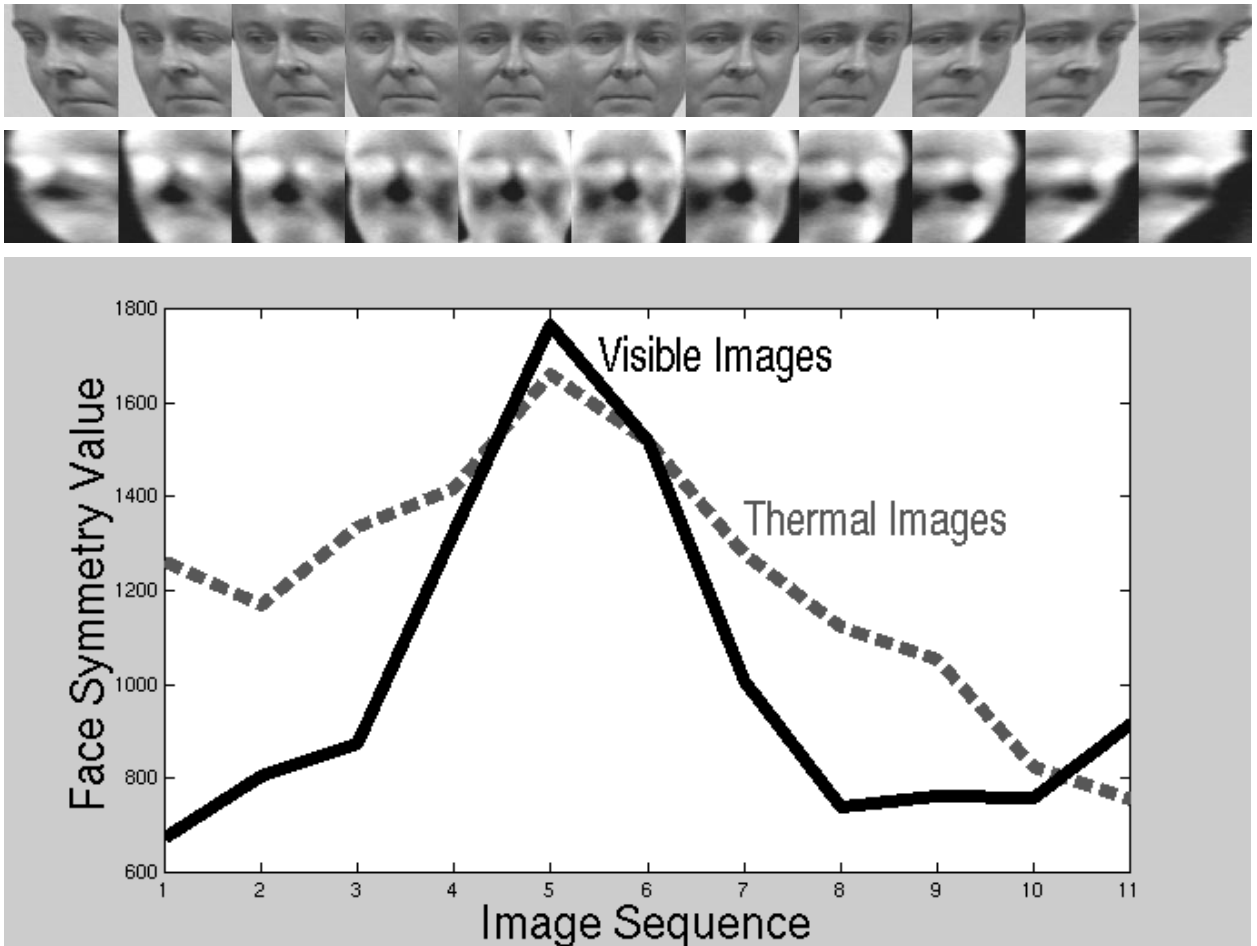


Figure 9: *Top: a video sequence of a subject being viewed from different angles. Middle: the corresponding thermal image sequence of the same subject. Bottom: the Edge Orientation Similarity plots (S-face) for both image sequences.*

References

- [1] P.N. Belhumeur, J.P. Jespanha, and D.J. Kriegman. Eigenfaces vs. fisherfaces: Recognition using class specific linear projection. *PAMI*, 19(7):711–720, July 1997.
- [2] R.M. Bilder, H. Wu, B. Bogerts, M. Ashtari, D. Robinson, M. Woerner, J.A. Lieberman, and G. Degreef. Cerebral volume asymmetries in schizophrenia and mood disorders: a quantitative magnetic resonance imaging study. *International Journal of Psychophysiology*, 34(3):197–205, December 1999.
- [3] C. M. Bishop. *Neural Networks for Pattern Recognition*. Clarendon Press, 1995. ISBN:0198538499.
- [4] J.D. Borod, E. Koff, S. Yecker, C. Santschi, and J.M. Schmidt. Facial asymmetry during emotional expression: Gender, valence and measurement technique. *Psychophysiology*, 36(11):1209–1215, 1998.
- [5] J.J. Collins and I.N. Stewart. Coupled nonlinear oscillators and the symmetries of animal gaits. *J. Nonlinear Science*, 3:349–392, 1993.
- [6] T.J. Crow. Schizophrenia as an anomaly of cerebral asymmetry. In K. Maurer, editor, *Imaging of the brain in psychiatry and related fields*. Springer-Verlag, 1993.
- [7] Editorial. Hemispheric asymmetry and psychopathology. *International Journal of Psychophysiology*, 34(3):183–185, December 1999.
- [8] K. Grammer and R. Thornhill. Human facial attractiveness and sexual selection: The role of symmetry and averageness. *Journal of Comparative Psychology*, 108:233–242, 1994.
- [9] T. Kanade, J.F. Cohn, and Y.L. Tian. Comprehensive database for facial expression analysis. In *4th IEEE International Conference on Automatic Face and Gesture Recognition*, Grenoble, March 1999. Publically available at http://www.ri.cmu.edu/projects/project_420.html.
- [10] Y. Liu, R.T. Collins, and W.E. Rothfus. Robust Midsagittal Plane Extraction from Normal and Pathological 3D Neuroradiology Images. *IEEE Transactions on Medical Imaging*, 20(3), March 2001.
- [11] Y. Liu, F. Dellaert, W.E. Rothfus, A. Moore, J. Schneider, and T. Kanade. Classification-driven pathological neuroimage retrieval using statistical asymmetry measures. In *International Conference on Medical Imaging Computing and Computer Assisted Intervention (MICCAI 2001)*. Springer, October 2001.

- [12] R. M. Mackie. Clinical differential diagnosis of cutaneous malignant melanoma. *Diagnosis and Management of Melanoma in Clinical Practice*, Kirkham, N. ed. London: Springer 1992.
- [13] L. Mealey, R. Bridgstock, and G.C. Townsend. Symmetry and perceived facial attractiveness: A monozygotic co-twin comparison. *Journal of Personality and Social Psychology*, 76(1):151–158, 1999.
- [14] O’Toole. The perception of face gender: The role of stimulus structure in recognition and classification. *Memory and Cognition*, 26(1):146,160, 1998.
- [15] C.K. Richardson, D. Bowers, R.M. Bauer, K.M. Heilman, and C.M. Leonard. Digitizing the moving face during dynamic displays of emotion. *Neuropsychologia*, 38(7):1028–1039, 2000.
- [16] R. Thornhill and S. W. Gangestad. Facial attractiveness. *Trans. in Cognitive Sciences*, 3(12):452–460, December 1999.
- [17] N.F. Troje and H.H. Buelhoff. How is bilateral symmetry of human faces used for recognition of novel views? *Vision Research*, 38(1):79–89, 1998.